

A Model for Shear Degradation of Lithium Soap Grease at Ambient Temperature

Yuxin Zhoua, Rob Bosmana and Piet M. Lugt

In this paper the shear degradation of lithium 12-hydroxy stearate grease will be measured using an in-house-developed Couette aging machine. In this device the shear rate is well defined. The aging is related to the generated entropy density, as described in Rezasoltani and Khonsari's work (Tribology Letters, Vol. 56, No. 2, pp. 197–204, 2014 and Ref. 11). The rheological properties of the aged samples were evaluated using a parallel-plate rheometer. The results showed that there are two aging phases with different degradation rates, i.e. — a progressive degradation phase at the early stage, followed by a rather slow deterioration afterwards. Based on this observation an aging equation was formulated to describe the aging behavior of lithium-thickened grease. Atomic force microscopy results of the fresh and aged greases showed that the variation in thickener microstructure provides a good explanation for the lithium grease degradation mechanism; under shear, the original fibrous network is progressively destroyed and becomes fragmented, leading to the loss of consistency and a change in the rheological properties.

Nomenclature

\bar{F}	Average load per stroke inside the grease worker (N)
f	Frequency for the oscillatory test (Hz)
G'	Storage modulus (Pa)
G''	Loss modulus (Pa)
h	Gap height of the aging machine (m)
K	Coefficient of degradation
L	Average thickener fiber length (μm)
L_{piston}	Piston displacement for one full stroke of the grease worker (m)
m	Degradation exponent
R^2	Goodness of fit
R_a	Surface roughness of the measuring plates (center line average, μm)
R_i	Radius of the rotating bob (m)
R_o	Radius of the stable housing case (m)
S_g	Generated entropy-per-unit volume during aging ($J/\text{mm}^3 K$)
S_g	Entropy generation rate-per-unit-volume during aging ($J = \text{mm}^3 Ks$)
S_{gw}	Generated entropy-per-unit-volume inside the grease worker ($J = \text{mm}^3 K$)
S_{ps}	Generated entropy-per-unit-volume during pre-shear ($J = \text{mm}^3 K$)
T_{gw}	Ambient temperature of the grease worker (K)
T_{ps}	Temperature during pre-shear (K)
V_a	Grease volume inside the Couette aging rig (mm^3)
V_{gw}	Grease volume inside the grease worker (mm^3)
W_{gw}	Work applied inside the grease worker (J)
Y_∞	Second-stage rheological value after infinitely long aging
Y_i	Initial rheological value for fresh grease
$\dot{\gamma}_a$	Aging shear rate (s^{-1})
$\dot{\gamma}_{ps}$	Shear rate for pre-shear (s^{-1})
Δ	Cone penetration depth (0.1 mm)
η_0	Zero shear rate viscosity (Pa·s)
η_∞	Grease viscosity after infinitely long aging (Pa·s)
η_b	Base oil viscosity (Pa·s)
η_i	Initial zero shear viscosity for fresh grease (Pa·s)
$\eta_{\dot{\gamma}_a}^l$	Grease viscosity at the aging shear rate $\dot{\gamma}_a$ (Pa·s)

τ	Shear stress within the aging gap (Pa)
τ_c	Crossover stress (Pa)
τ_{ps}	Shear stress during pre-shear (Pa)
τ_{y-HB}	Yield stress obtained from Herschel-Bulkley model (Pa)
τ_{y-osc}	Yield stress obtained from the oscillatory strain sweep test (Pa)
ϕ	Thickener volume fraction
ω	Rotational speed of the aging machine (rad/s)

Introduction

Grease is a widely applied lubricant, mostly used in rolling bearings. It is a multi-phase system consisting of three parts: thickener (3–30%), base oil (70–90%), and additives (Ref. 1). As a semi-solid material, grease has a high consistency that prevents leakage and creates a reservoir of lubricant inside the bearing. However, when subjected to the severe conditions within a rolling bearing, grease will undergo high shear, possibly causing deterioration. The degradation of this grease is usually reflected by the loss of its original consistency (softening), possibly yielding leakage from the bearing and, hence, starvation. It may also lead to continuous churning and high temperature. Both cases result in a reduced life of the bearing (Ref. 1). It is therefore valuable to investigate the mechanism of grease degradation and to develop predictive models for this.

Generally, the degradation of grease is classified as chemical or mechanical aging. This article focuses on the mechanical aging of lithium 12-hydroxystearate-thickened grease. This type of grease takes the major share of the worldwide industrial grease market and is widely applied in rolling bearings due to its wide temperature applicability, relatively good mechanical stability, water-resistant properties, and low cost (Ref. 1).

The most straightforward way to study grease aging is to obtain data from field tests directly, where the grease is worked in a real bearing (Ref. 2). Such field practice requires

Grease	NLGI	Thickener	Volume fraction of the thickener ϕ	Shape and average size of thickener	Base oil	Base oil viscosity at 25°C η_b
Li/M	3	Lithium 12-hydroxy stearate	14%	Twisted fiber $L \approx 2 \mu\text{m}$	Mineral oil	0.23 Pa·s
Li/SS	2	Lithium 12-hydroxy stearate	16%	Twisted fiber $L \approx 2 \mu\text{m}$	Semi-synthetic	0.07 Pa·s

a long timescale study. For example, in the work of Lundberg and Höglund (Ref. 3), aged samples were collected from the wheel bearings of railway wagons after years of service. Another drawback of this method is the fact that it is practically impossible to estimate the exact aging conditions—that is, the shear stress/rate, temperature, and time—to which the sample was subjected during operation.

Currently, there are two standards for measuring grease degradation. One is the mechanical stability test, where normal load and shear are applied; this is considered particularly meaningful in the situation where the bearing is subjected to vibrations and where the grease is continuously thrown back into the tracks. A typical mechanical stability test is the roll stability test (ASTM D 1831), where grease is sheared between a heavy roller (with a lead core) and a hollow rotating cylinder at an elevated temperature (generally 80°C). It was found that this test can be used to simulate the practical working conditions in automobile wheel bearings (Refs. 4–5) and in rolling bearings in railway wagons (Refs. 6–7). The other test is the shear stability test, where only shear is applied. This is considered important for bearings running under relatively stable working conditions. When subjected to continuous shear, it is observed that shear degradation of the grease results in the release of oil and thus provides lubricant replenishment (Refs. 8–9). In the “grease worker” (ASTM D 217), which consists of a closed cylinder and a piston plate with a number of holes, the grease is sheared through the holes during a well-defined number of strokes (usually 10,000 or 100,000 strokes).

The drawback of the two ASTM aging methods mentioned above is that the applied shear condition is not well defined, which makes it difficult to use these methods for the development of predictive aging models. To measure aging as a function of shear and time, a modified Couette rheometer was used in the shear measurements of grease (Ref. 10). Rezasoltani and Khonsari (Ref. 11) made use of a parallel-plate rheometer for the long-term shear tests of lithium-thickened grease. Aging in a rheometer provides a controlled aging process where the rheology can directly be measured as a function of time. However, the disadvantage of a parallel-plate configuration is that the shear field within the gap is not uniform, resulting in an inhomogeneous aging condition. In addition, in the current rheological study, leakage was observed in the parallel-plate geometry due to the centrifugal forces, and in the open Couette configuration due to the Weissenberg effect (Ref. 12). Hence, at some point during aging the measurement will become inaccurate. Therefore, more robust test rigs are required.

Rezasoltani and Khonsari (Ref. 11; p. 200) discovered a linear relationship between the energy input and the grease properties during grease aging tests using a parallel-plate rheometer. They mentioned that this “linear correlation remains

valid, regardless of the applied shear rate or the grease temperature.” This was verified using a journal bearing mounted between two rolling bearings to provide a uniform film along the circumference of the journal bearing (hence the journal bearing was not loaded) and a modified grease worker. The experimental data of the journal bearing test rig showed a slight deviation from the linear relation obtained from the rheological measurements at the end of their experiments, which was ascribed to grease separation from the journal and a slippage effect during the tests.

The aim of the current study is twofold: the first objective is to follow up on the work of (Ref. 11). The influence of grease mechanical degradation on its shear stability will be evaluated under similar aging conditions using lithium-thickened grease samples, but with an increased aging period, thus increasing the total amount of entropy generated. The second goal is to study the underlying mechanism responsible for the aging of lithium grease.

To achieve the first task, fresh greases will be sheared in an in-house-made Couette aging machine at specific shear rates for a set period of time. Then the grease is sampled and its rheological properties are measured. Though lubricating grease can be considered chemically stable at low temperatures (Ref. 13), Fourier transform infrared spectroscopy (FTIR) measurements will be performed for both the fresh and aged samples to confirm this. The physical processes occurring during mechanical degradation will be studied by measuring the change in the microstructure of the aged samples using atomic force microscopy (AFM).

Materials and Method

Two commercial lithium-thickened greases—Li/M and Li/SS—were used. Information on their composition is presented in Table 1 (Ref. 14).

Aging Tests

Test rig. In the current study, the grease has been aged by means of applying specific shear rates for a set period, similar to what is done in a grease worker. However, the shear rate is now well defined. Normal load (or hydrostatic pressure) will not be applied at first (so only the shear stability of the grease will be studied). The grease should be aged in a closed system, where leakage is avoided. Another requirement for the new test rig is that a sufficient amount of aged grease can be collected for subsequent rheological tests.

The new test rig (called a Couette aging test rig) is shown (Fig. 1). The basic concept is analogous to a cylindrical viscometer in that the grease is sheared between a stationary housing case and a rotating bob that is driven by a motor and a belt transmission. The shear rate exerted over the grease can thus be calculated based on the input rotational speed and the geometry of the aging head. The temperature dur-

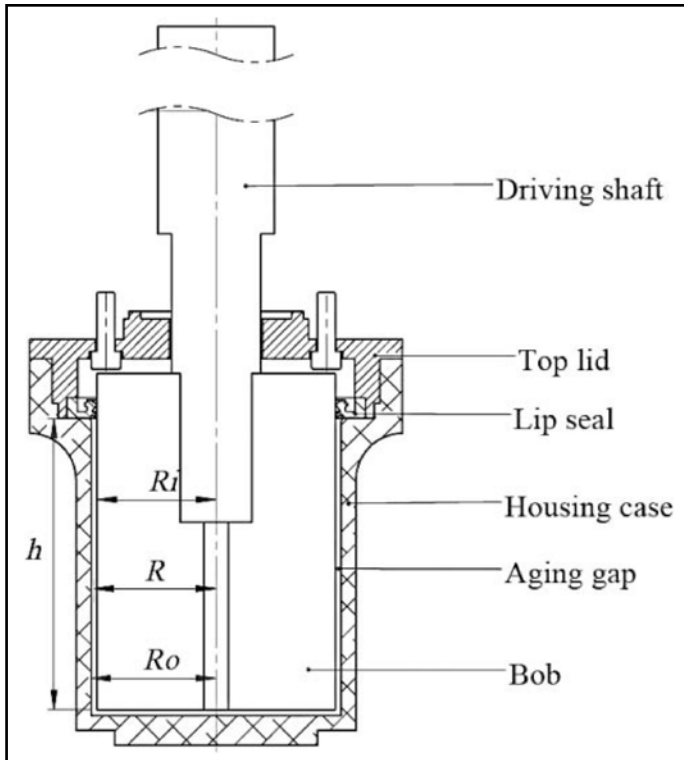


Figure 1 Couette aging test rig.

ing the aging procedure is captured by the thermocouple at the end of the aging head. To prevent grease leakage due to the Weissenberg effect, a lip seal is mounted on top of the aging gap. The rig was designed for a grease sample volume of $V_a = 5.1 \times 10^4 \text{ mm}^3$ for each aging test (where $R_i = 40 \text{ mm}$; $R_o = 42 \text{ mm}$; and $h = 100 \text{ mm}$; leaving a 2-mm gap between the rotating bob and the housing case).

Aging Condition

The aging rotational speeds are selected such that the imposed shear rates are similar to those applied on the aging tests performed by (Ref. 11). The input rotational speeds, corresponding shear rates, and aging periods are listed in Table 2.

Sampling. The lip seal (Fig.1) generates a moderate amount of frictional heat, leading to a temperature gradient in the vertical direction. Together with possible thickener-oil separation due to shear, the thickener of the aged grease might no longer be evenly distributed inside the aging gap. The aged samples were therefore mixed for 500 strokes in an in-house-made grease worker before the rheological measurements were performed.

Rheological Measurements

Rheological measurements were performed for the fresh and aged grease samples using an MCR 501 Anton-Paar rheometer with parallel plate configuration. The viscosity was measured by steady-state flow curve measurements. In addition, oscillatory strain sweep measurements were performed to measure the grease's viscoelastic properties.

Preparation. There are three major concerns during rheological measurements: wall slip, loading history, and edge effects. To reduce the influence of wall slip, measuring plates with rough surfaces are recommended (Refs.15–16). Therefore the plates were roughened by sand-blasting (top plate: $R_a = 1.5 \mu\text{m}$; bottom plate: $R_a = 2.3 \mu\text{m}$). Then, to minimize the initial deviation induced by the placing and loading procedure, the grease samples were first deposited on the bottom plate and the top plate, descended at a controlled speed until the measure position was reached, leaving a 1-mm measuring gap. Thereafter, pre-shear following a DIN standard (Ref.17) was applied (pre-shear at $\dot{\gamma}_s = 100 \text{ s}^{-1}$ for 60 s at 25°C). Subsequently, the accumulated grease at the plate periphery was carefully removed with a spatula. See Figure 2 for the loading and pre-shear procedure.

As a thixotropic material, regeneration of the thickener microstructure occurs after shearing the grease (Refs. 16 and 18). Therefore, before data collection, sheared grease is left to rest for a sufficient relaxation time. This duration will depend on the grease microstructure, thickener concentration, pre-shear condition, etc., and can be determined by a time sweep measurement.

Here the time dependency of the shear modulus was recorded while imposing an oscillatory shear well within the linear viscoelastic regime (the applied shear is sufficiently small to not disrupt the grease properties). The detailed procedure is as follows: after pre-shear, a 2-h oscillatory test was applied at a constant shear stress of 10 Pa, oscillation frequency $f = 1 \text{ Hz}$, and temperature $25 \pm 1^\circ\text{C}$. Both Li/M and Li/SS show a similar trend: the highest recovery of G' takes place during the first hour of relaxation and the value levels out afterwards, which is in agreement with the literature (Ref. 18).

As a consequence, a relaxation time of 60 min was applied prior to the tests. The application of pre-shear and sufficient relaxation guarantees that the deviation in the following rheological results can be controlled within a 10% spread, which satisfies the requirements for grease rheological measurement specified in DIN 51810-2 (Ref. 17).

Flow curve and oscillatory strain sweep measurement. Once the sample was prepared following the procedure described above, rheological tests were conducted. The flow curve measurement was performed at $25 \pm 1^\circ\text{C}$ with the shear rate increasing from 10^{-8} s^{-1} up to 10^2 s^{-1} . The oscillatory strain

Table 2 Aging condition for Li/M and Li/SS.						
Rotational speed (rpm)	Shear rate $\dot{\gamma}_a$ (s^{-1})	Aging time (h)				
83	174	5	25	50	100	200
125	261	5	25	50	100	200
166	348	5	25	50	100	200



Figure 2 Loading and preshear procedure.

sweep measurement was performed at $25 \pm 1^\circ\text{C}$ at a frequency of 1Hz, with the shear strain sweeping from $10^{-3}\%$ to $10^3\%$. Each type of measurement was repeated at least twice. The repeatability of both flow curve and oscillatory strain sweep measurements was calculated based on the deviation from the average value of the duplicated test results (Table 3).

Deviation	Flow curve measurement	Oscillatory strain sweep
Li/M Li/SS	$\pm 7.1\%$ of the mean $\pm 4.6\%$ of the mean	$\pm 7.8\%$ of the mean $\pm 10\%$ of the mean

Data Process

Rheological output. Two representative results for both flow curve and oscillatory strain sweep measurements are presented in Figure 3. As shown in Figure 3a, the flow curve measurement shows shear thinning of grease under continuously increasing shear. A zero-shear viscosity $\eta_0 = 8.9 \times 10^5 \text{ Pa} \cdot \text{s}$ was obtained using the Cross model fit (Ref. 19). In Figure 3b the storage modulus G' , loss modulus G'' , and crossover stress τ_c are obtained from the plot directly; the yield stress τ_{-osc} was calculated using the method described by Cyriac et al. (Ref. 20).

Entropy generation calculation. The entropy generated per unit volume during aging (S_g) will be calculated based on the estimated frictional energy generated by the grease and recorded temperature during the aging process following the approach proposed by (Ref. 11).

If chemical reactions are neglected, the mechanical degradation of grease is such a slow process that “the major portions of the system are in homogeneous states that change slowly enough with time” (Ref. 21, p. 3). In this case, the entropy generated is equal to the accumulated energy divided by the aging temperature, which is produced through the absorption of heat (Ref. 22).

The recorded temperature showed that during aging, the variation in aging temperature was less than 2°C and the change in the system’s internal energy was negligible com-

pared to the energy accumulated during aging. Therefore, the accumulated energy is equal to the work exerted on the grease; that is, the integration of the grease frictional torque and the rotational speed over the aging time (Ref. 21). The entropy generated per unit volume S_g can thus be expressed as:

$$S_g = \frac{\text{work}/V_a}{\text{Temperature}} = \frac{\int \text{Torque} \cdot \omega dt}{\text{Temperature} \times V_a} \quad (1)$$

Here, ω is the input rotational speed, t is the aging time, and V_a is the grease volume inside the Couette aging rig. In the current rig, the torque generated by the grease cannot be recorded directly and is calculated using the shear stress acting over the area $2\pi R h$ at a distance R from the central axis (Ref. 23):

$$\text{Torque} = 2\pi R h \tau \cdot R = 2\pi R^2 h \tau = 2\pi R^2 h \dot{\gamma} \eta | \dot{\gamma}_a \quad (2)$$

Here, $\dot{\gamma}_a$ is the applied shear rate presented in Table 2 and $\eta | \dot{\gamma}_a$ is the grease’s apparent viscosity at the aging shear rate. The geometrical notations (Eq. 2) are shown (Fig. 1). During the aging process the grease’s apparent viscosity is not constant. To obtain the viscosity at the aging shear rate ($\eta | \dot{\gamma}_a$), grease samples were collected after each aging period. Flow curve measurements were performed on these samples, from which the $\eta | \dot{\gamma}_a$ was estimated from a Cross model fit; an example of this $\eta | \dot{\gamma}_a$ is displayed as the aging point in Figure 3a.

In this way the torque during the aging process can be calculated periodically. Figure 4 shows an example of the torque distribution where Li/M was aged at 83 rpm for 200 h. The accumulated energy and the corresponding entropy generation density can be calculated by integrating the torque distribution over the aging period (Eq. 1).

The work and entropy induced by the 500-strokes mixture within the grease worker was calculated based on (Ref. 11); the entropy generated inside the grease worker is equal to the applied work W_{gw} divided by the ambient temperature T_{gw} ; where W_{gw} is the product of the average load and the piston distance for one stroke multiplied by the number of strokes

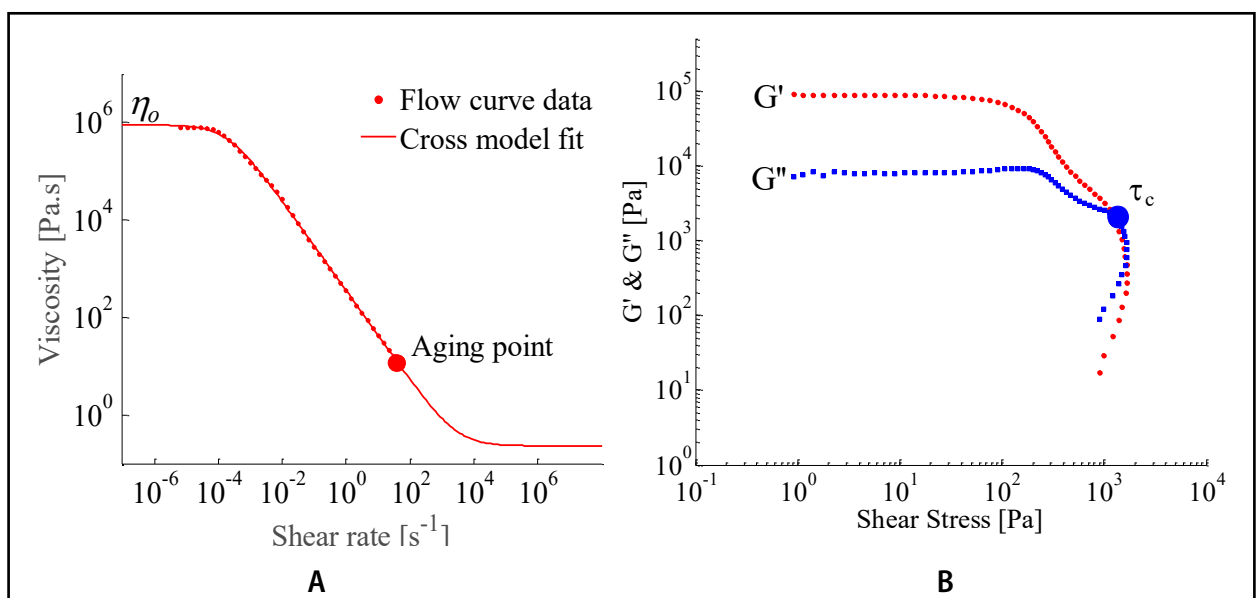


Figure 3 Typical rheological output obtained from an aged sample: (a) flow curve test and (b) oscillatory strain sweep test.

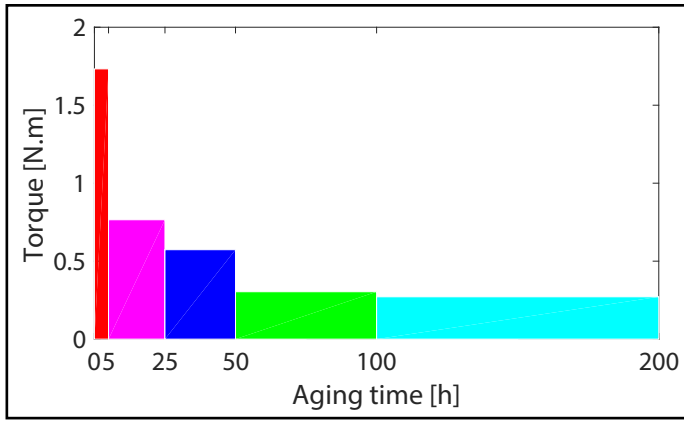


Figure 4 Calculated torque distribution for LiM aged at 83 rpm for 200 h.

(500).

The average load F for one stroke (both tension and compression) during the pre-shearing, recorded by a load cell mounted beneath the cylinder of the grease worker, was $F=8:75$ N for fresh Li/M and $F=6:20$ N for fresh Li/SS. The piston displacement for one full stroke was measured as $L_{piston}=5.68 \times 10^2$ m. The volume of the grease sheared inside the cylinder was $V_{gw}=1.23 \times 10^4$ mm³ and the ambient temperature $T_{gw}=25^\circ\text{C}=298$ K. The entropy generation per unit volume during the 500 strokes is thus calculated as:

$$S_{gw} = \frac{W_{gw}/V_{gw}}{T_{gw}} = \frac{500 \bar{F} \cdot L_{piston}}{V_{gw} \cdot T_{gw}} \quad (3)$$

For Li/M, $S_{gw}=6.8 \times 10^{-5}$ J/mm³K; and for Li/SS, $S_{gw}=4.8 \times 10^{-5}$ J/mm³K.

In addition, the pre-shear procedure before the rheological measurement creates entropy. As specified in the Preparation section, the grease sample will be pre-sheared at $\dot{\gamma}_{ps}=100$ s⁻¹ for 60 s at 25°C. Based on (Ref. 11), the entropy generation density during the pre-shear procedure S_{ps} within the rheometer can be expressed as:

$$S_{ps} = \dot{\gamma}_{ps} \cdot \frac{\int \tau_{ps} dt}{T_{ps}} \quad (4)$$

where

$\dot{\gamma}_{ps}$ is the shear rate applied during pre-shear ($\dot{\gamma}_{ps}=100$ s⁻¹), τ_{ps} is the shear stress recorded during pre-shear, t is time, and T_{ps} is the temperature during pre-shear (controlled at $T_{ps}=25^\circ\text{C}$).

For fresh Li/M, $S_{ps}=1.0 \times 10^{-5}$ J/mm³K and for fresh Li/SS, $S_{ps}=5.2 \times 10^{-5}$ J/mm³K.

The entropy generation density during the sample preparation, i.e. $-S_{gw}+S_{ps}$ is at least 100 times smaller than that generated during the aging test, and can therefore be neglected. For the following study, only the entropy density generated during the aging tests S_g will be taken into account.

Aging mechanism investigation. The microstructure of the grease thickener is studied using atomic force microscopy (AFM) in dynamic tapping mode, which

is widely applied on soft biological samples and greases (Refs. 24–26). The advantage of AFM over conventional scanning electron microscopy and transmission electron microscopy is that the soap structure can be observed without the need to remove the oil (Refs. 27–28). In addition, the sample preparation is limited to smearing a small volume of grease on a flat glass plate.

Results and Discussion

Verification of chemical reaction. The FTIR spectra (limited wave number range of 4,000–650 cm⁻¹) of fresh and aged Li/M are presented (Fig. 5). As an inhomogeneous material, grease thickener is not evenly distributed, resulting in the amplitude variation at zone 3,500–3,230 cm⁻¹ (- OH bond), 1,580 cm⁻¹ (COO⁻ asymmetric stretch), and 1,459 cm⁻¹ (- CH deformation), which indicates the difference in thickener concentration. However, no extra peaks are found between the fresh and aged samples' spectra; therefore, based on the detection accuracy of the current FTIR device, chemical reactions are not observed during the aging tests. A similar result was found for Li/SS. This was to be expected, because the maximum value of the recorded temperature during aging was low for the lithium-thickened greases (52°C for Li/M and 48°C for Li/SS). Thus the entropy calculation approach from (Ref. 11) can be applied (Ref. 21).

Thermodynamic characterization of grease mechanical degradation. In this section the results from aging grease in the Couette aging rig will be presented and compared to those found by (Ref. 11). As specified in the previous Methodology section, we used the same shear rates and the same definition of entropy as (Ref. 11). However, Rezasoltani and Khonsari (Ref. 11) used the net penetration value as a response parameter, a measure of the consistency of a grease sample. To compare the current rheological values to (Ref. 11) results, a relationship between the penetration value and the yield stress was applied (Ref. 29):

$$\tau_{y-HB} = 3 \times 10^{10} \cdot \Delta^{-3.17} \quad (5)$$

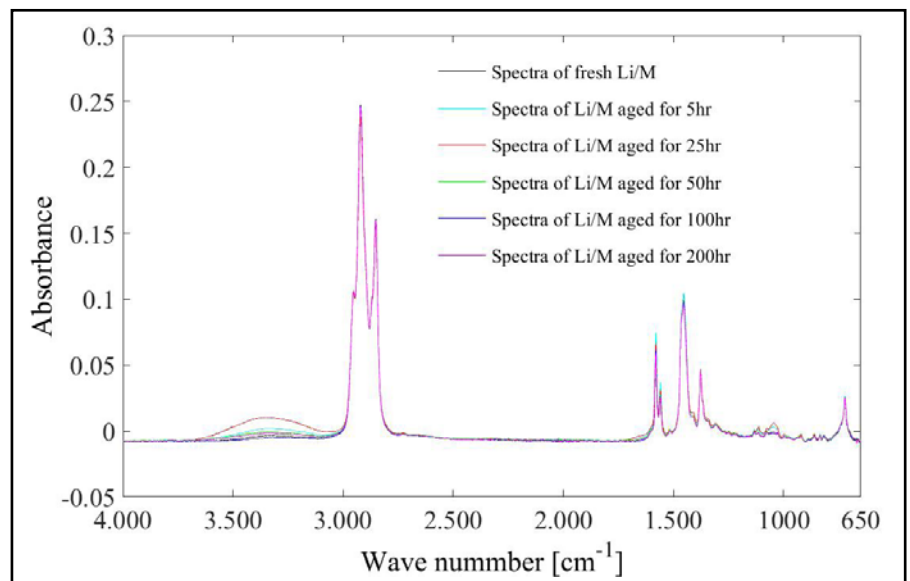


Figure 5 FTIR spectra of fresh and aged Li/M.

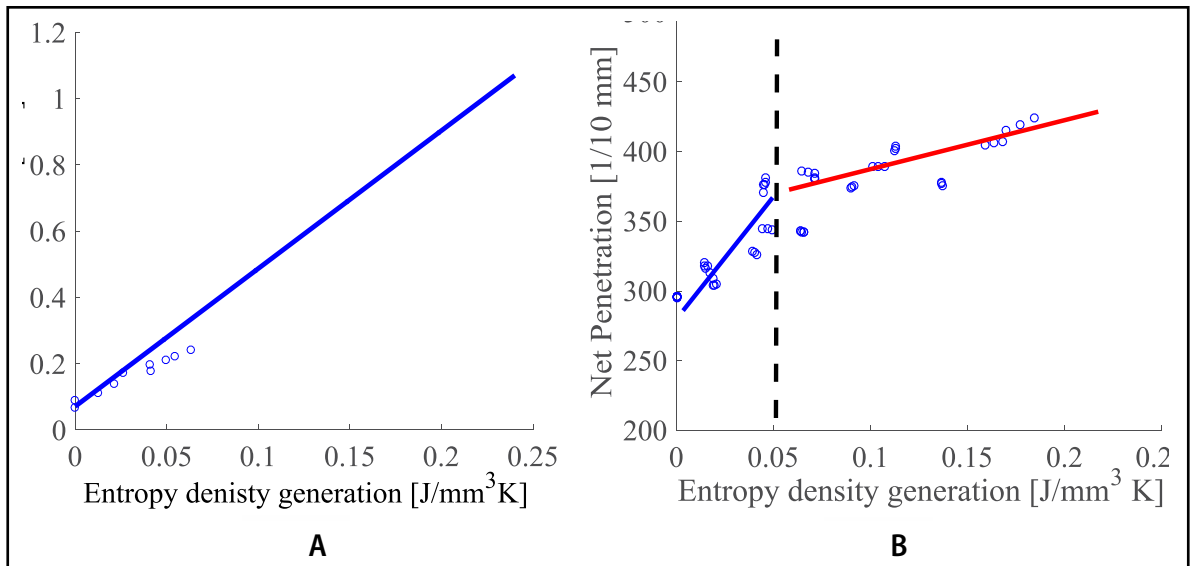


Figure 6 Comparison of penetration values against entropy generation density during the aging process: (a) reproduced from Rezasoltani and Khonsari (11) and (b) results from the current study (Li/M).

where

$\tau_{\gamma-HB}$ is the yield stress obtained from the flow curve data based on Herschel-Bulkley model (Ref. 29), and Δ is the cone penetration depth (10^{-1} mm).

Rezasoltani and Khonsari did not use the standard ASTM method to measure the penetration depth; however, it is assumed that they scale similarly. As listed in Table 2, 15 samples were prepared and examined for the effects of each type of grease on aging. The calculated penetration depth of Li/M against entropy generation density is presented in Figure 6b, together with the data rebuilt from the results of (Ref. 11) (Fig. 6a).

In the present case (Fig. 6b) a linear relationship can be observed in the early stage of the aging process; i.e. — $S_g < 0.05 \text{ J/mm}^3\text{K}$. At this point the degradation behavior changes. Again a linear behavior is observed — but with a different slope. The results from (Ref. 11) also show a deviation from the linear fit at higher values of entropy density; however, this was less pronounced. The aging behavior (Fig. 6b) can be translated into a fast deterioration phase at an early stage and a slower deterioration phase afterwards.

Figures 7 and 8 show the variation in the zero-shear viscosity with entropy generation per unit volume for Li/M and Li/SS, respectively, when subjected to three different shear rates. Again, two phases can be seen: a progressive degradation in the first stage followed by a rather slow deterioration afterwards. This agrees with the penetration depth variation against entropy generation per unit volume illustrated in Figure 6. Similar trends were also found from the literature survey (Refs. 30–32).

The viscosity versus entropy generation trend of lithium-thickened grease is similar to the viscosity versus shear rate (shear thinning) behavior of lubricating greases. At relatively low shear (or energy), the grease

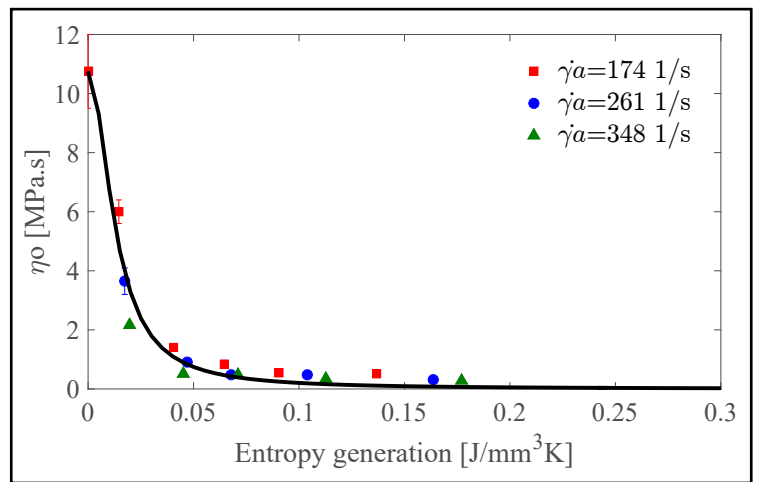


Figure 7 Zero-shear viscosity variation versus entropy generation density for Li/M.

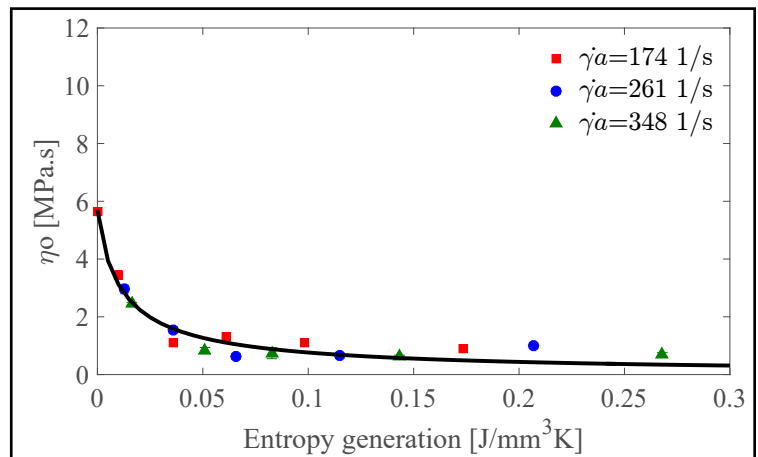


Figure 8 Zero-shear viscosity variation versus entropy generation density for Li/SS.

has an initial high viscosity (here indicated as η_i). However, when mechanical degradation starts, the sample begins to soften; after being subjected to a certain amount of entropy ($S_g=0.05 \text{ J/mm}^3\text{K}$), the viscosity levels out again with a weak degradation rate.

Therefore the formula of the Cross equation (Ref. 19), which is used to describe shear thinning behavior, was borrowed to describe the relationship between the variation in zero-shear viscosity and the entropy generation density during aging:

$$\eta_\infty = \frac{\eta_i - \eta_\infty}{1 + K \cdot S_g^m} + \eta_\infty, \tag{6}$$

where

η_i is the initial zero-shear viscosity for fresh samples; and η_∞ is the viscosity for infinitely long shearing, which is calculated using Batchelor's equation, $\eta_\infty = \eta_b (1 + 2.5 + 6.2^2)$ (Ref. 33); the base oil viscosity η_b and the phase volume are tabulated in Table 1; S_g is the generated entropy-per-unit volume during aging; K is the coefficient of degradation; and m is the exponent of degradation.

Equation 6 fits the data obtained from all three shear rates very well ($R^2=0.99$) (Figs. 7-8). This model has also been applied to the other three selected rheological properties: storage modulus G' , crossover stress τ_c , and yield stress τ_{y-osc} from the oscillatory test in the form of Equation 7 — called here the “grease aging equation”:

$$Y = \frac{Y_i - Y_\infty}{1 + K \cdot S_g^m} + Y_\infty, \tag{7}$$

where

Y represents the rheological properties, Y_i represents the initial rheological value for fresh grease, Y_∞ represents the second-stage value for the longtime-aged sample, and K and m are the coefficient of degradation and the exponent of degradation, respectively.

Each grease will have its own aging master curve, or grease aging equation, with its specific parameters (Table 4).

		Y_i	Y_∞	K	m	R^2
η_0 (Pa·s)	Li/M	1.1×10^7	0.34	4.5×10^3	1.9	0.99
	Li/SS	5.7×10^6	0.11	5.0×10^3	0.89	0.99
G' (Pa)	Li/M	9.0×10^4	2.2×10^3	5.9×10^3	2.2	0.99
	Li/SS	8.0×10^4	9.3×10^3	1.0×10^3	1.6	0.98
τ_c (Pa)	Li/M	1.2×10^3	1.0×10^2	4.0×10^3	2.2	0.99
	Li/SS	7.2×10^2	2.7×10^1	4.0×10^2	1.2	0.99
τ_{y-osc} (Pa)	Li/M	70	3	1.8×10^1	1.1	0.91
	Li/SS	50	6	6.6×10^2	1.9	0.95

Grease aging mechanism. The generation of entropy demonstrates a dissipative process, which brings disorder to the system and, in this case, probably the collapse of the grease's microstructure. According to the literature, the consistency and rheological properties of fibrous structured greases are closely related to the geometry and distribution of the network structure formed by the fibers (Refs. 4-5; 25 and 34).

As shown in Figure 6b, there are two aging phases with different degradation rates. According to (Ref.35), the entropy generation rate is closely related to the system degradation rate. Here the system degradation rate is measured by the changes in rheological properties per unit of time (macro-

scopically) and the change in the thickener network (microscopically). The entropy generation rate per unit of volume can be expressed as:

$$\dot{S}_g = \frac{\text{Torque} \times \omega / V_a}{\text{Temperature}}. \tag{8}$$

The entropy generation rate per unit volume and the degradation rate of the zero-shear viscosity η_0 for Li/M during the aging tests are plotted against aging time in Figure 9. AFM measurements of the grease were taken at different points in time and are also shown (Fig. 9). The drawings are interpretations of the AFM pictures that will help in the explanation of the results.

Figure 9 shows the entropy generation rate, rheology, and microstructure of Li/M during aging. Although only the degradation rate for zero-shear viscosity is shown, the plots for crossover stress, storage modulus, and yield stress are very similar. The thickener microstructure for fresh Li/M is visualized as a twisted fibrous network where the fibers are typically 0.1–0.2 μm wide and up to 3 μm long. Initially, the sample shows high consistency. When the mechanical degradation is initiated, energy is dissipated into the system (high S_g), disrupting the network crosslinks and aligning the fibers (as presented in the first two drawings and AFM results). This results in a fast degradation in grease properties. This stage can be characterized by the coefficient of degradation K (values of K are listed in Table 4) and it ends when the fibrous network becomes fragmented (until 50 h) (Fig. 9).

After this fast degradation stage the aged sample becomes a mixture of particle-like microfragments of thickener (with an average length of 0.1 μm) dispersed in the oil, and the deterioration process slows down (the degradation rate is approaching zero after 100 h of aging (Fig. 9). Such behavior suggests that once the fibrous structure is completely destroyed, the grease rheology will become stable. With the deceleration of the aging process, the entropy generation rate becomes smaller and remains constant.

However, the existence of microfragments or nanosized thickener fibers (Ref. 34) still gives the aged grease a higher consistency compared to that of the bled oil (see the second-stage values Y_∞ for the aged samples presented in Table 4). According to the R2F bearing tests performed (Ref. 9), small volumes of viscous liquid were found in the cage pockets — which was assumed to lubricate the rolling track. Infrared spectroscopy showed that this lubricant was a mixture of oil and thickener, and more viscous liquid was found along with the running. Such viscous liquid can be considered as the aged grease at the second stage, where it has both better flowability — compared to the fresh grease (for lubricant replenishment) — and higher viscosity compared to the base oil (for film construction).

Spiegel, et al. (Ref. 31) described the fragmented thickener as spherical particles and modeled the second-stage mechanical aging using a Wöhler curve. Their theory suggests that when subjected to continuous shear, these spherical particles start rolling and the governing aging mechanism is fatigue. Considering the results (Fig. 9), in the second stage, the thickener structure has become fragmented during the

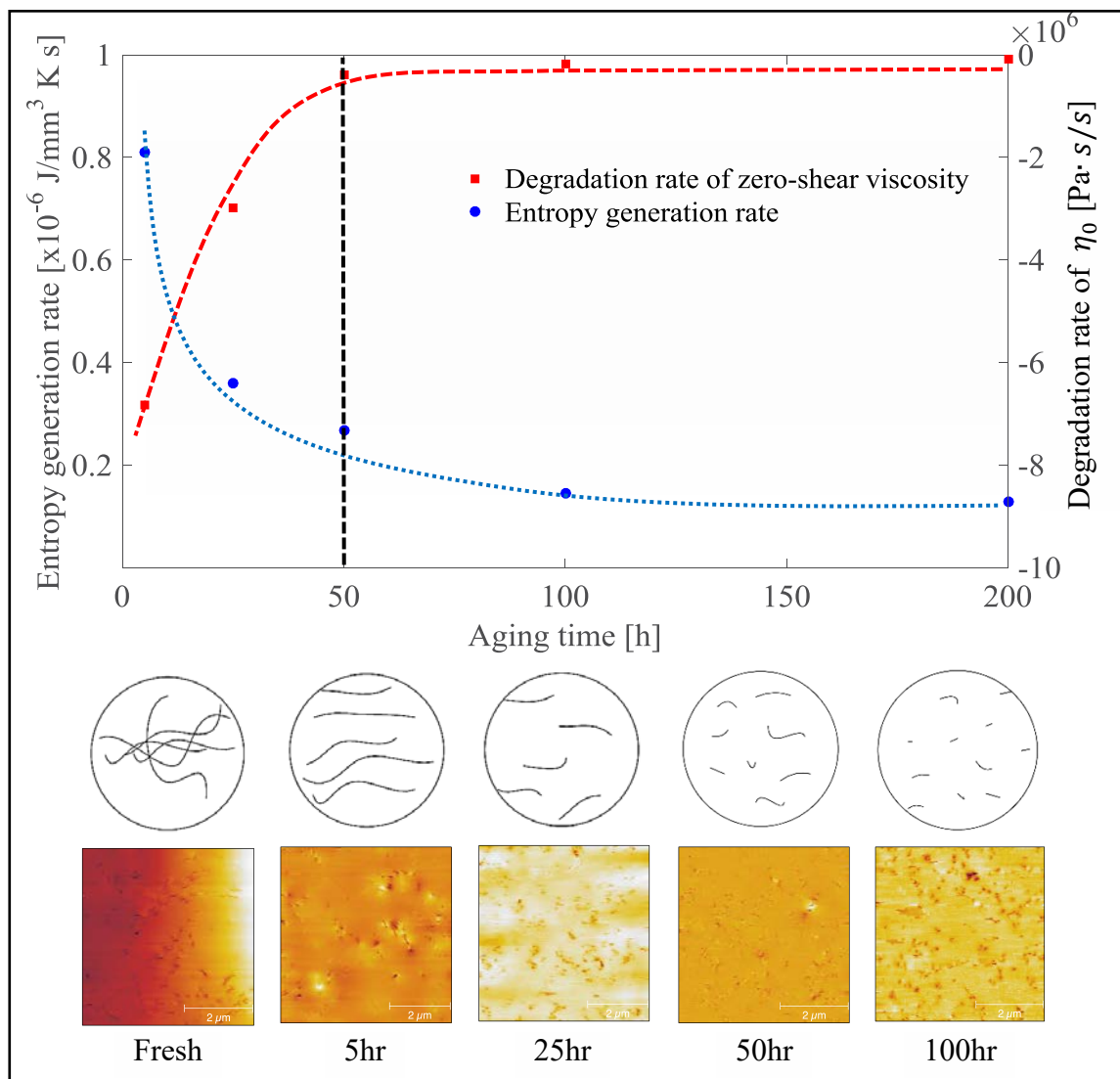


Figure 9 Aging of Li/M; cartoon and AFM results for different aging stages.

second phase and the grease ages at a slower rate, compared to the first aging phase. Currently the grease rheology during aging is assumed to end up at an infinite value Y_{∞} (Table 4; Figs. 7–8). A similar aging mechanism is also observed for Li/SS. To confirm Spiegel's (Ref. 31) theory, prolonged aging tests will be needed.

Conclusion

In this study the mechanical shear degradation of lithium-thickened grease was evaluated using an in-house-developed aging rig and a commercial rheometer. It was found that this grease loses its original consistency during aging and shows a two-phase aging behavior. In the first phase, primarily reorientation and breakage of the thickener network take place, resulting in a progressive drop in the grease's rheological properties. After this, the aging is dominated by the breakage of smaller fiber fragments and the grease degrades at a much slower rate (but currently considered stable). A grease shear aging equation (Eq. 7) was introduced to describe such two-phase behavior. By making use of the entropy concept, this equation is capable of covering the change in grease's rheo-

logical properties when aged at different shear rates. This aging behavior is closely related to the entropy generation rate and the change in the thickener network during the aging process: due to breakage of the thickener structure, grease degrades and the aging rate is positively correlated to the entropy generation rate. According to (Ref. 11) the shear aging at various shear rates and temperatures can be described by a single (master) curve using the entropy concept. In the current study the entropy concept was confirmed using aging at different shear rates; the current test rig does not allow for variance of the aging temperature. It is therefore recommended to further study the impact of temperature on the shear aging behavior of grease.

Funding. The authors thank SKF Engineering and Research Centre for the financial support of this work. **PTE**

References

1. Lugt, P. M. *Grease Lubrication in Rolling Bearings*, 2013, New York, NY, Wiley & Sons.
2. Salomonsson, L., G. Stang and B. Zhmud. "Oil/Thickener Interactions and Rheology of Lubricating Greases," *Tribology Transactions*, 50(3), 2007, pp 302–309.

3. Lundberg, J. and E. Högglund. "A New Method for Determining the Mechanical Stability of Lubricating Greases," *Tribology International*, 2000, 33(3), pp 217-223.
4. Bondi, A., A.M. Cravath, R.J. Moore and W.H. Peterson. "Basic Factors Determining the Structure and Rheology of Lubricating Grease," *The Institute Spokesman*, 1950, 13(12), pp 12-18.
5. Moore, R. J. and A.M. Cravath. "Mechanical Breakdown of Soap-Based Greases," *Industrial & Engineering Chemistry*, 1951, 43(12), pp 2892-2897.
6. Lundberg, J. "Grease Lubrication of Roller Bearings in Railway Wagons. Part 1: Field Tests and Systematic Evaluation to Determine the Optimal Greases," *Industrial Lubrication & Tribology*, 2000, 52 (1), pp 36-43.
7. Lundberg, J. and S. Berg. "Grease Lubrication of Roller Bearings in Railway Wagons. Part 2: Laboratory Tests and Selection of Proper Test Methods," *Industrial Lubrication & Tribology*, 2000, 52(2), pp 76-85.
8. M'erieux, J., S. Hurley, A.A. Lubrecht and P.M. Cann. "Shear Degradation of Grease and Base Oil Availability in Starved EHL Lubrication," *Tribology Series*, 2000, 38, pp 581-588.
9. Cann, P. M., J.P. Doner, M.N. Webster and V. Wikstrom. "Grease Degradation in Rolling Element Bearings," *Tribology Transactions*, 2001, 44(3), pp 399-404.
10. Paszkowski, M. "Identification of the Thixotropy of Lithium Greases," *16th International Colloquium Tribology*, 2008, Esslingen, Germany.
11. Rezasoltani, A. and M.M. Khonsari. "On the Correlation between Mechanical Degradation of Lubricating Grease and Entropy," *Tribology Letters*, 2014, 56(2), pp 197-204.
12. Schramm, G. "A Practical Approach to Rheology and Rheometry," 1994, Haake: Karlsruhe, Germany.
13. Ito, H., M. Tomaru and T. Suzuki. "Physical and Chemical Aspects of Grease Deterioration in Sealed Ball Bearings," *Lubrication Engineering*, 1988, 44(10), pp 872-879.
14. Cyriac, F., P. Lugt, R. Bosman, C. Padberg and C. Venner. "Effect of Thickener Particle Geometry and Concentration on the Grease EHL Film Thickness at Medium Speeds," *Tribology Letters*, 2016, 61(2), pp 1-13.
15. Czarny, R. "The Influence of Surface Material and Topography on the Wall Effect of Grease," *Lubrication Science*, 2002, 14(2), pp 255-274.
16. Paszkowski, M. "Assessment of the Effect of Temperature, Shear Rate and Thickener Content on the Thixotropy of Lithium Lubricating Greases," *Proceedings of the Institution of Mechanical Engineers - Part J: Journal of Engineering Tribology*, 2013, 227(3), pp 209-219.
17. Deutsches Institut für Normung. "Testing of Lubricants — Determination of Shear Viscosity of Lubricating Greases by Rotational Viscosimeter — Part 1: System of Cone/Plate," 2007.
18. Paszkowski, M., S. Olsztyń'ska-Janus and I. Wilk. "Studies of the Kinetics of Lithium Grease Microstructure Regeneration by Means of Dynamic Oscillatory Rheological Tests and FTIR-ATR Spectroscopy," *Tribology Letters*, 2014, 56(1), pp 107-117.
19. Cross, M. M. "Rheology of Non-Newtonian Fluids: A New Flow Equation for Pseudo-Plastic Systems," *Journal of Colloid Science*, 1965, 20(5), pp 417-437.
20. Cyriac, F., P.M. Lugt and R. Bosman. "On a New Method to Determine the Yield Stress in Lubricating Grease," *Tribology Transactions*, 2015, 58(6), pp 1021-1030.
21. Rezasoltani, A. and M. Khonsari. "Reply to Comment by Chung on 'On the Correlation between Mechanical Degradation of Lubricating Grease and Entropy,'" *Tribology Letters*, 2015, 60(1), pp 1-4.
22. Tolman, R. and C. P.C. Fine. "On the Irreversible Production of Entropy," *Reviews of Modern Physics*, 1948, 20(1), pp 51-77.
23. Godec, D., A.Y. Malkin and A.I. Isayev. "Rheology — Concepts, Methods & Applications," *Polimeri*, 2006, 27(1), pp 282-283.
24. Hoefnagels, J. P. M. "Overview of Microscopic Characterization Techniques," Eindhoven, The Netherlands, Eindhoven University of Technology.
25. Sanchez, M. C., J. Franco, C. Valencia, C. Gallegos, F. Urquiola and R. Urchegui. "Atomic Force Microscopy and Thermo-Rheological Characterization of Lubricating Greases," *Tribology Letters*, 2011, 41(2), pp 463-470.
26. Paszkowski, M. and S. Olsztyń'ska-Janus. "Grease Thixotropy: Evaluation of Grease Microstructure Change Due to Shear and Relaxation," *Industrial Lubrication & Tribology*, 2014, 66(2), pp 223-237.
27. Hurley, S. and P.M. Cann. "Examination of Grease Structure by SEM and AFM Techniques," *NLGI Spokesman*, 2001, 65(5), pp 17-26.
28. Delgado, M. A., J.M. Franco, C. Valencia, E. Kuhn and C. Gallegos. "Transient Shear Flow of Model Lithium Lubricating Greases," *Mechanics of Time-Dependent Materials*, 13(1), pp 63-80.
29. Spiegel, K., J. Fricke and K. Meis. "Coherence between Penetration and Flow Limit of Greases," *Tribologie und Schmierungstechnik*, 1991, 38(6), pp 326-331.
30. Plint, M. and A. Alliston-Greiner. "A New Grease Viscometer: A Study of the Influence of Shear on the Properties of Greases," *NLGI Spokesman*, 1992, 56(2), pp 7-15.
31. Spiegel, K., J. Fricke and K. Meis. "Die Fließeigenschaften von Schmierfetten in Abhängigkeit von Beanspruchung, Beanspruchungsdauer und Temperatur," 2000, *International Colloquium Tribology*: Esslingen, Germany.
32. Kuhn, E. "Experimental Grease Investigations from an Energy Point of View," *Industrial Lubrication & Tribology*, 1999, 51(5), pp 246-251.
33. Barnes, H. A., J.F. Hutton and K. Walters. *An Introduction to Rheology*, Amsterdam, 1989, The Netherlands, Elsevier.
34. Yoshiyuki, S., N. Yusuke, I. Yusuke, S. Hiroki and F. Yukitoshi. "Characterization of Nano Size Thickener Fiber in Grease by SAXS," *World Tribology Congress*, 18-13 September, Torino, Italy.
35. Bryant, M. D., M.M. Khonsari and F.F. Ling. "On the Thermodynamics of Degradation," *Proceedings of the Royal Society of London A: Mathematical, Physical and Engineering Sciences*, 2008, 464 (2096).

Yuxin Zhou is a Ph.D. candidate working since 2014 in the Surface Technology and Tribology group at the University of Twente (Netherlands), focusing on the aging mechanism of lubricating grease. He received his BSc degree in marine engineering at Dalian Maritime University (China), studying bearing film thickness measurement, and was awarded an MSc degree in advanced mechanical engineering at Imperial College London (UK), projecting the bearing surface optimization.



Rob Bosman studied mechanical engineering and tribology at the University of Twente in The Netherlands (MSc. 2007, Ph.D. 2011). He then worked at Pentair FairBanks-Nijhuis for 2 years as an R&D and reliability engineer, after which he returned to the university as an assistant professor and is currently an associate professor. Along with his professorship Bosman since 2014 has worked part-time at Shell Rijswijk R&D as a research coordinator.



Piet M. Lugt studied mechanical engineering and tribology at the University of Twente in The Netherlands (MSc. 1988, Ph.D. 1992). He then worked at the Technical University of Delft in chemistry and vehicle dynamics until 1995 when he joined SKF Research, where he has fulfilled several positions in tribology and lubrication — presently as a senior scientist. He has also been a part-time professor at Luleå Technical University, Sweden (2005-2008) and since 2011 at the University of Twente. Lugt is the author of *Grease Lubrication in Rolling Bearings* — a book regarded as a major contribution to the industry.



For Related Articles Search

at www.powertransmission.com